

An evaluation of candidate geomagnetic field models for the 10th generation of IGRF

Susan Macmillan and Anna Droujinina, British Geological Survey, 12 November 2004

1. Introduction

For the 10th generation IGRF a total of seven main-field (MF) candidate models for 2005.0 and eight secular-variation (SV) candidate models for 2005.0-2010.0 were submitted for evaluation to IAGA Working Group V-MOD. The candidate models were submitted by Danish Space Research Institute in collaboration with NASA and Newcastle University (DSRI-NASA-Newcastle model, group A), by US National Geophysical Data Center and GeoForschungsZentrum (NGDC-GFZ model, group B), British Geological Survey (BGS model, group C) and Institute of Terrestrial Magnetism, Ionosphere and Radio Wave Propagation (IZMIRAN model, group D). The models are compared with one another in terms of root mean square differences and mean differences at the surface of the earth.

2. Model Descriptions

A summary of the data and modelling methods used to generate each model is given in Table 1. Where a group has submitted several models their preferred model is indicated by an asterisk. Note that for the secular variation models Lowes selected A3 rather than A1 in his evaluation.

Table 1 Summary of models

<i>Group</i>	<i>Model</i>	<i>Organization</i>	<i>Data</i>	<i>Notes</i>
<i>Main-field models</i>				
A	IGRF-A1*	DSRI/NASA/ Newcastle	Ørsted and CHAMP Aug 2000-Aug 2004	quadratic
	IGRF-A2	DSRI/NASA/ Newcastle	Ørsted and CHAMP Jul 2002-Aug 2004	linear
B	IGRF-B1	NGDC/GFZ	CHAMP Aug 2000-Jul 2004	quadratic
	IGRF-B2	NGDC/GFZ	Ørsted Apr 1999-Jul 2004	quadratic
	IGRF-B3*	NGDC/GFZ	Ørsted and CHAMP Apr 1999-Jul 2004	quadratic
C	IGRF-C1	BGS	Ørsted, CHAMP and observatory hourly mean data 1999.0-2004.35	quadratic
D	IGRF-D1	IZMIRAN	CHAMP time span not specified	linear
<i>Secular-variation models</i>				
A	SV-A1-2005*	DSRI/NASA/ Newcastle	Ørsted and CHAMP Aug 2000-Aug 2004	dB/dt at 2005.0, extrapolated from quadratic
	SV-A2-2005	DSRI/NASA/ Newcastle	Ørsted and CHAMP Jul 2002-Aug 2004	dB/dt from linear
	SV-A3-2007.5	DSRI/NASA/ Newcastle	Ørsted and CHAMP Aug 2000-Aug 2004	dB/dt at 2007.5, extrapolated from quadratic
B	SV-B1-2007.5	NGDC/GFZ	CHAMP Aug 2000-Jul 2004	dB/dt at 2005.0, extrapolated from quadratic
	SV-B2-2007.5	NGDC/GFZ	Ørsted Apr 1999-Jul 2004	dB/dt at 2007.5, extrapolated from quadratic
	SV-B3-2007.5*	NGDC/GFZ	Ørsted, CHAMP and observatory annual mean data (1995-Jul 2004)	dB/dt at 2007.5, extrapolated from quadratic
C	SV-C1-2007.5	BGS	Ørsted, CHAMP and observatory hourly and annual mean data (18**-.2004.35)	dB/dt at 2007.5, extrapolated from quadratic+linear prediction filters applied to observatory dB/dt series
D	SV-D1-2005	IZMIRAN	CHAMP May 2001-Aug 2004	Natural orthogonal components, dB/dt from linear

3. Inter-Model Comparisons

The candidate models have been compared with each other using root mean square (RMS) differences of F on a sphere of radius 6371.2 km using the Lowes-Mauersberger estimate (Figures 1-4), plotting differences on the surface of earth (Figures 5-10) and computing mean differences for X, Y and Z on 2° latitude/longitude grid on the surface of earth (Tables 2-5). The RMS differences confirm those of Figure 1a, Table 4, Figure 3a and Table 7 of Lowes' evaluation and are here presented in Figures 1-4 as *mean* RMS differences (this differs from Lowes Figure 1b and 3b where all model differences are used to compute MEAN4, here there is no common mean). Like Lowes, comparisons are made between all candidate models and a selection of candidate models. The same selection is used here for the MF models but for the SV models A1 is used instead of A3 as this is the model preferred by the authors.

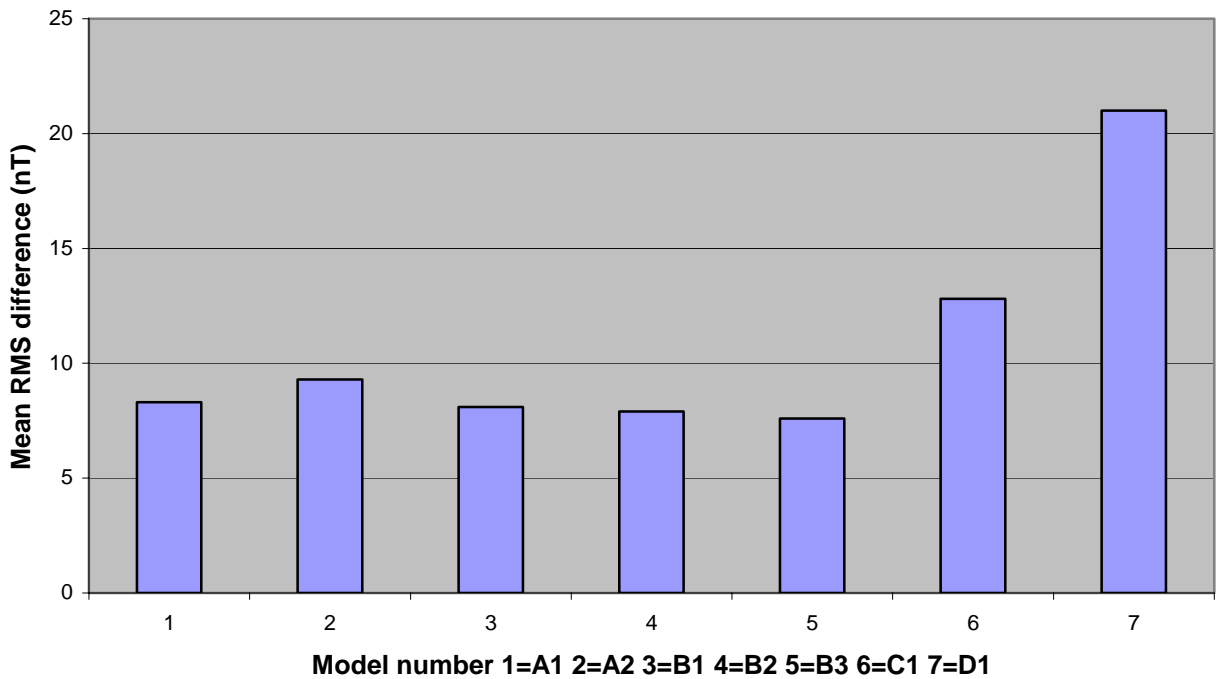


Figure 1

It can be seen in Figure 1 that MF models C1 and D1 are different from the others.

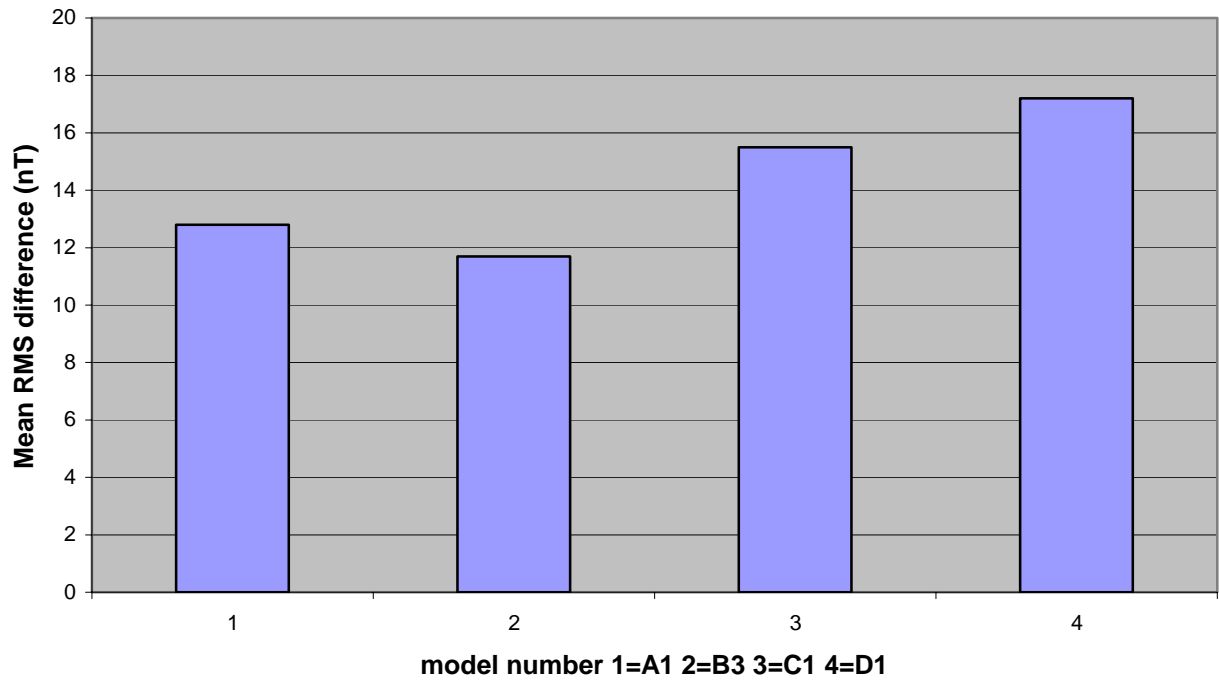


Figure 2

From Figure 2 it can be seen that MF model B3 is most similar to the other models and that D1 is least similar.

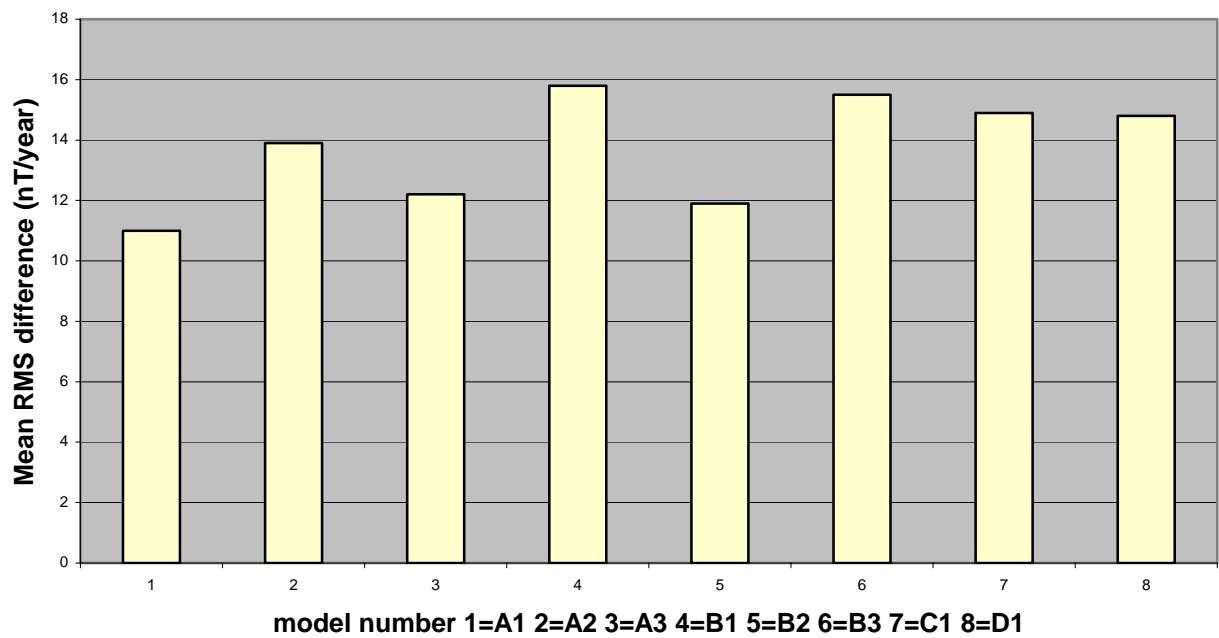


Figure 3

From Figure 3 it can be seen that there is quite a range in the SV models, from about 11 - 16 nT/year.

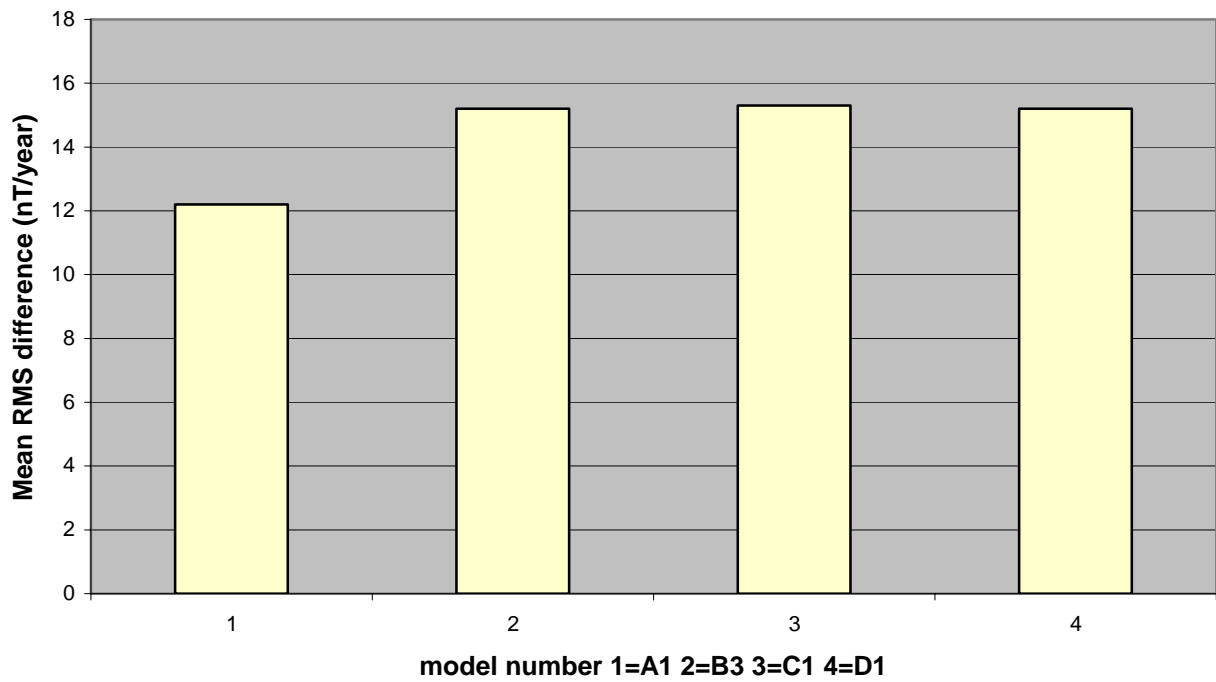


Figure 4

When only the selection of SV models is considered, it can be seen that the range reduces to about 12 - 15 nT/year. Model A1 is most similar to the other models.

In the following plots of differences we restrict ourselves to the four MF models.

Differences between MF-IGRF models, A1 and B3, at Earth surface (C.I. = 2 nT)

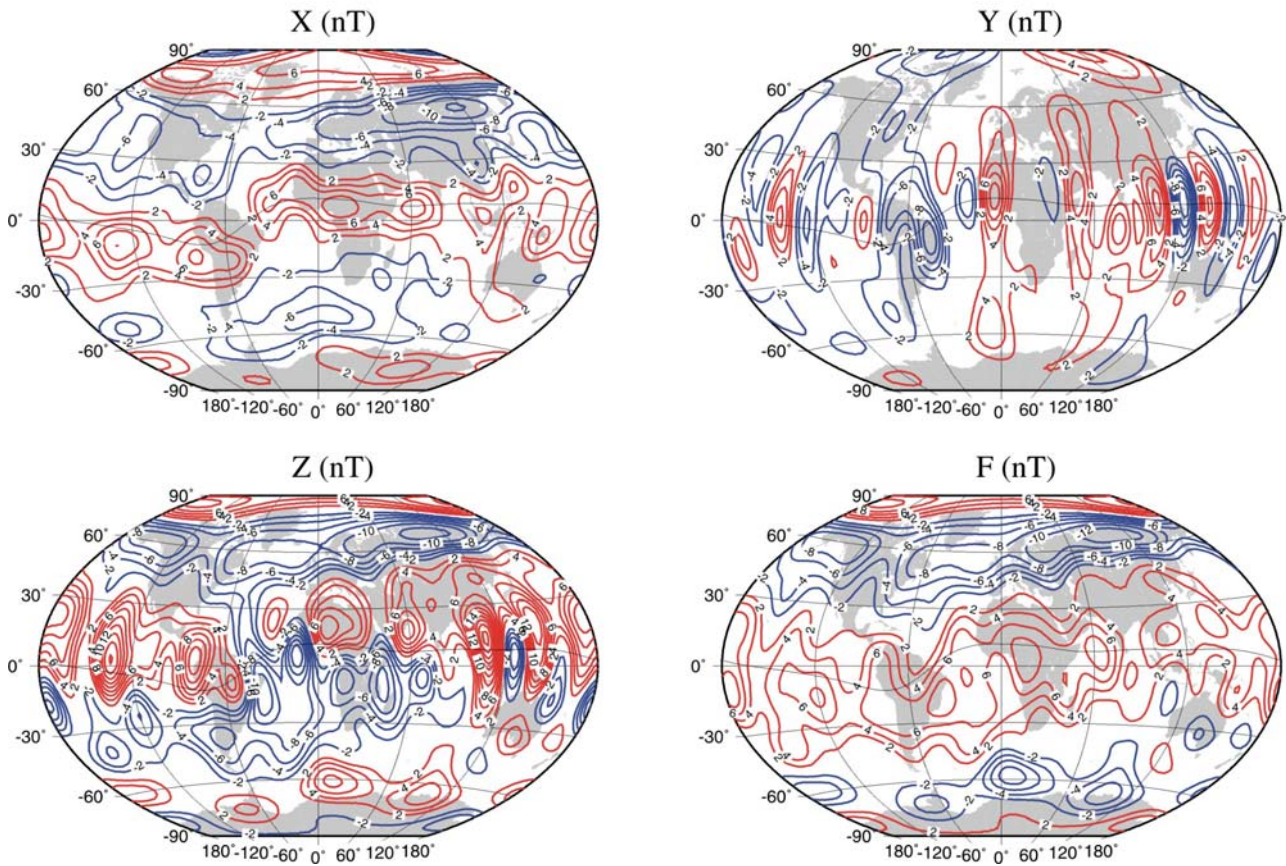


Figure 5

From Figure 5 it can be seen that the most significant pattern in the differences is that dependent on latitude with 4 zeros, i.e. the degree 4 zonal coefficients. Either A1 or B3 is the source of this. The first A1 coefficient is -29556.5 and this model therefore should therefore have an ionospheric correction, a likely source for this pattern, applied only once (the first version of A1 apparently had the correction applied twice).

Differences between MF-IGRF models A1 and C1, at Earth surface (C.I. = 2 nT)

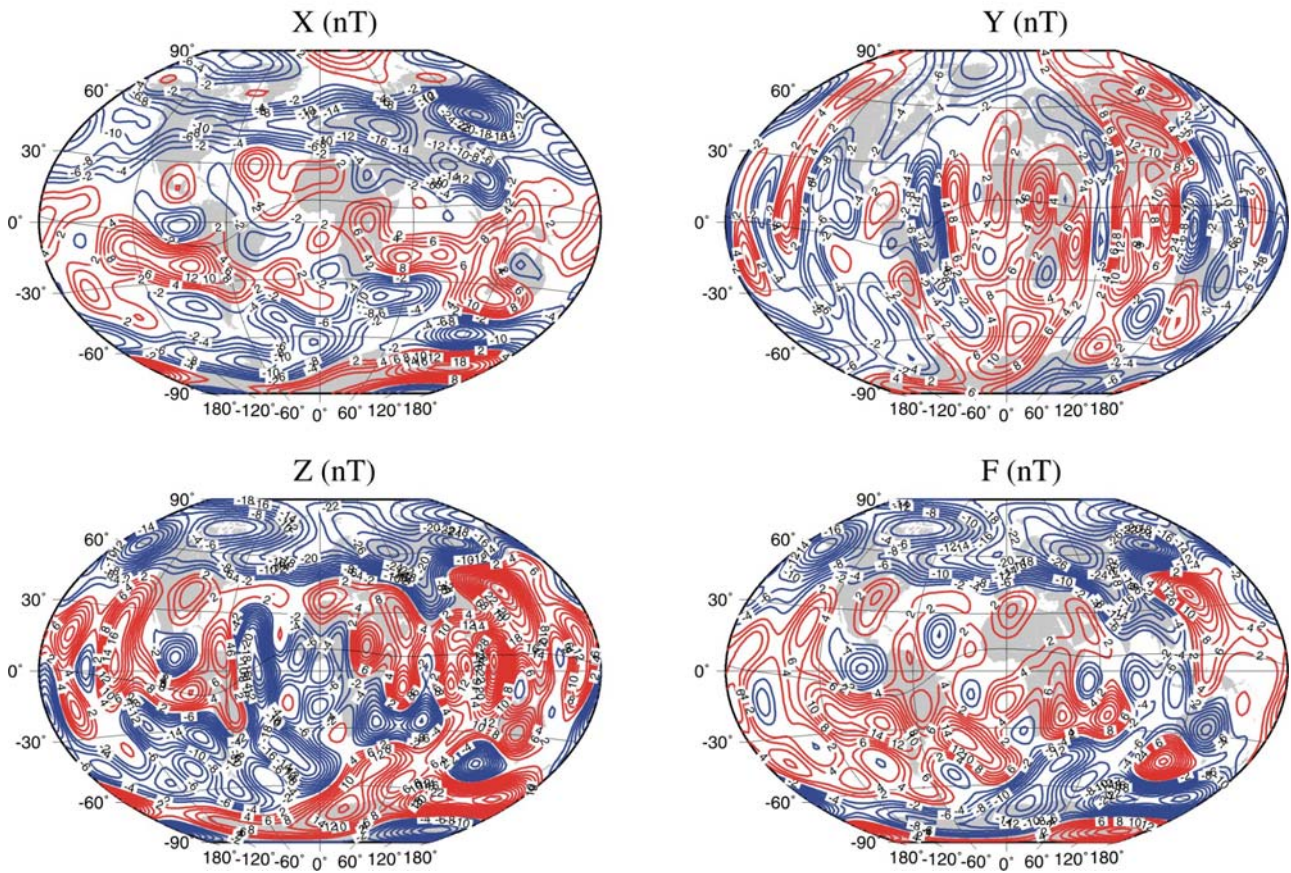


Figure 6

The pattern of differences is slightly more random in Figure 6 than in Figure 5, but there are still signs of a degree 4 zonal pattern. The amplitude of the differences is larger than in Figure 5 and, in addition, there are large differences at northern latitudes. The common model in Figure 5 and 6 is A1.

Differences between MF-IGRF models, A1 and D1, at Earth surface (C.I. = 2 nT)

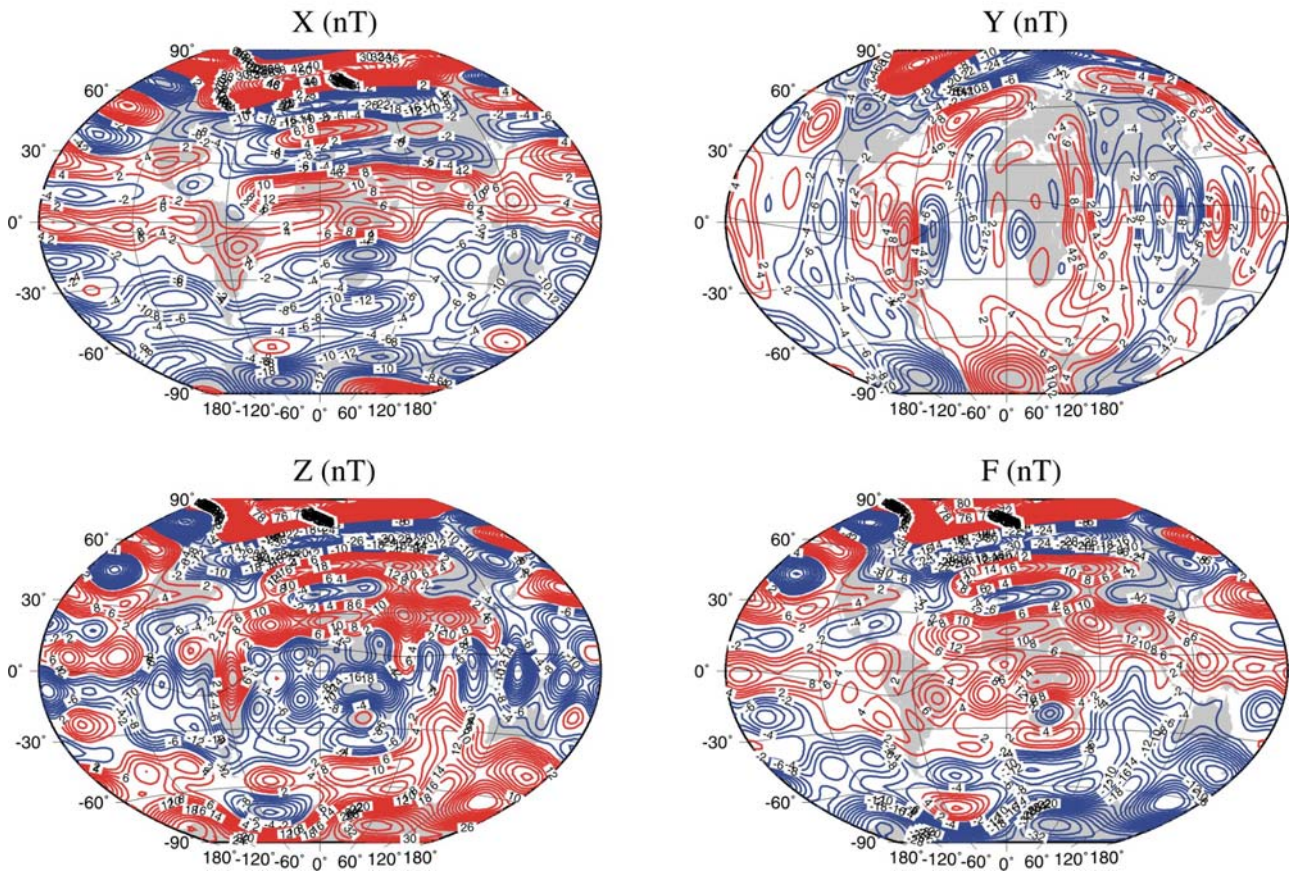


Figure 7

The most significant feature of Figure 7 is the large differences in the polar regions. There are signs of a degree 4 zonal pattern, almost certainly coming from A1.

Differences between MF-IGRF models, B3 and C1, at Earth surface (C.I. = 2 nT)

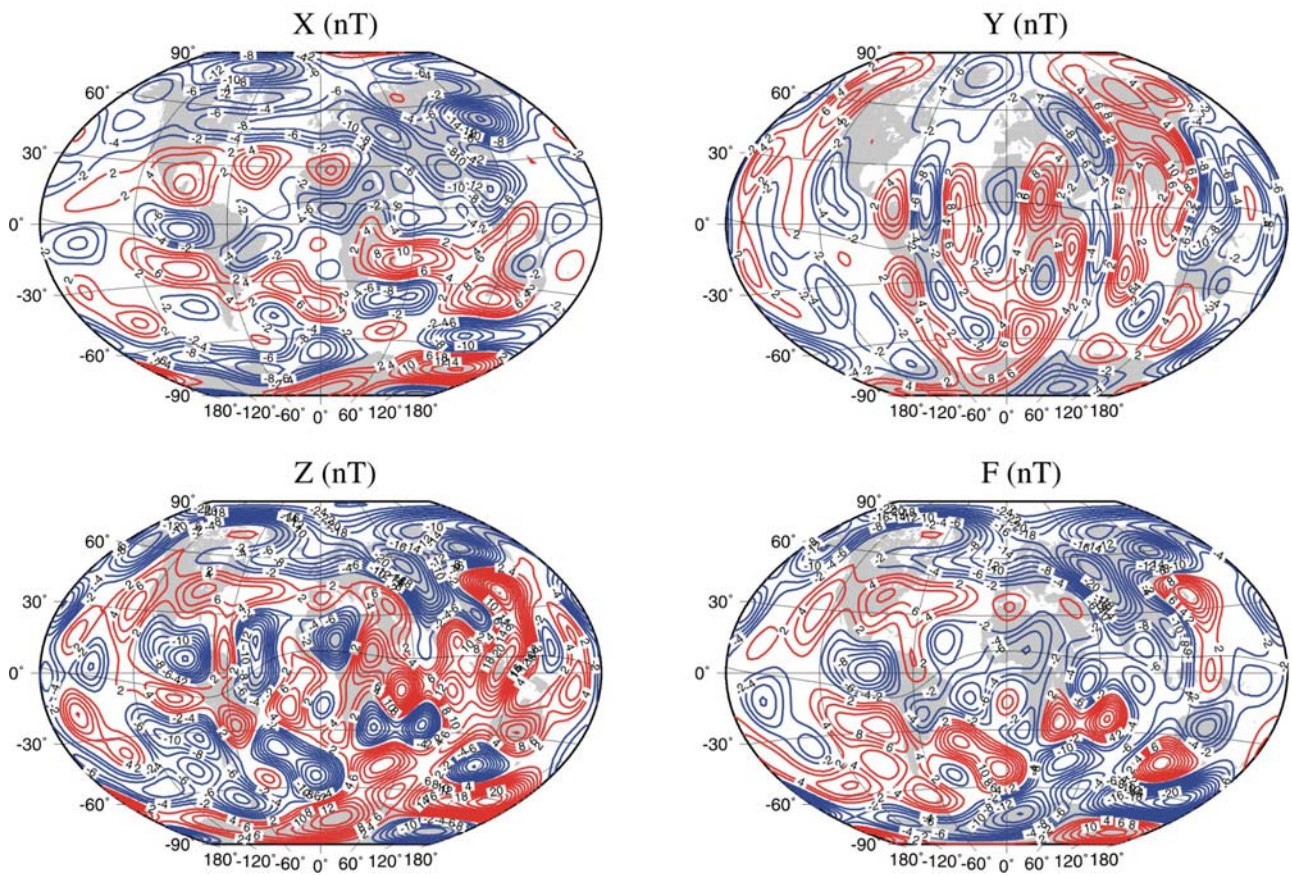


Figure 8

Apart from the differences at northern latitudes, the patterns in Figure 8 are reasonably random. The common model in Figures 6 and 8 is C1.

Differences between MF-IGRF models, B3 and D1, at Earth surface (C.I. = 2 nT)

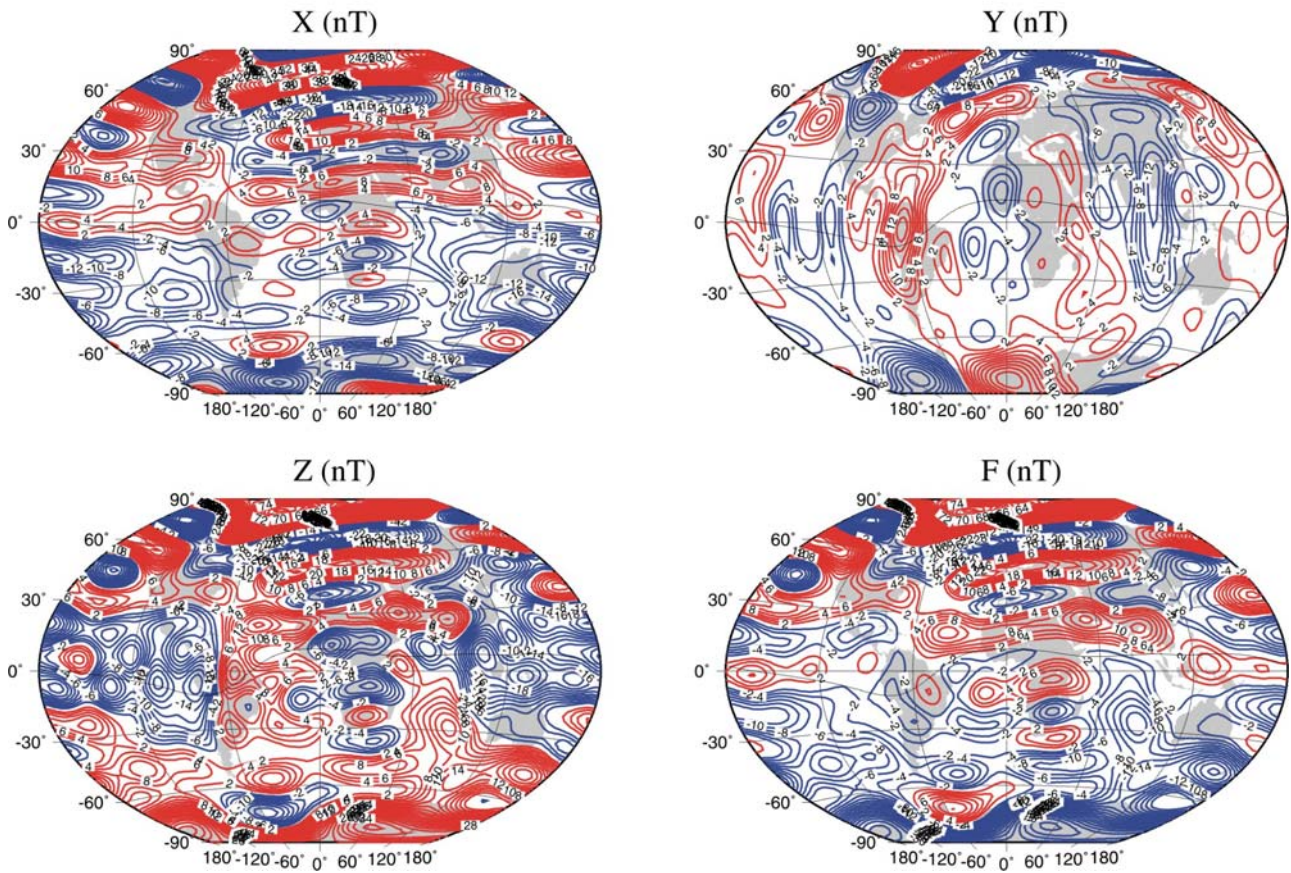


Figure 9

The amplitude of the differences is large in Figure 9 and there are large differences in the polar regions, the northern region being affected more than the southern region.

Differences between MF-IGRF models, C1 and D1, at Earth surface (C.I. = 2 nT)

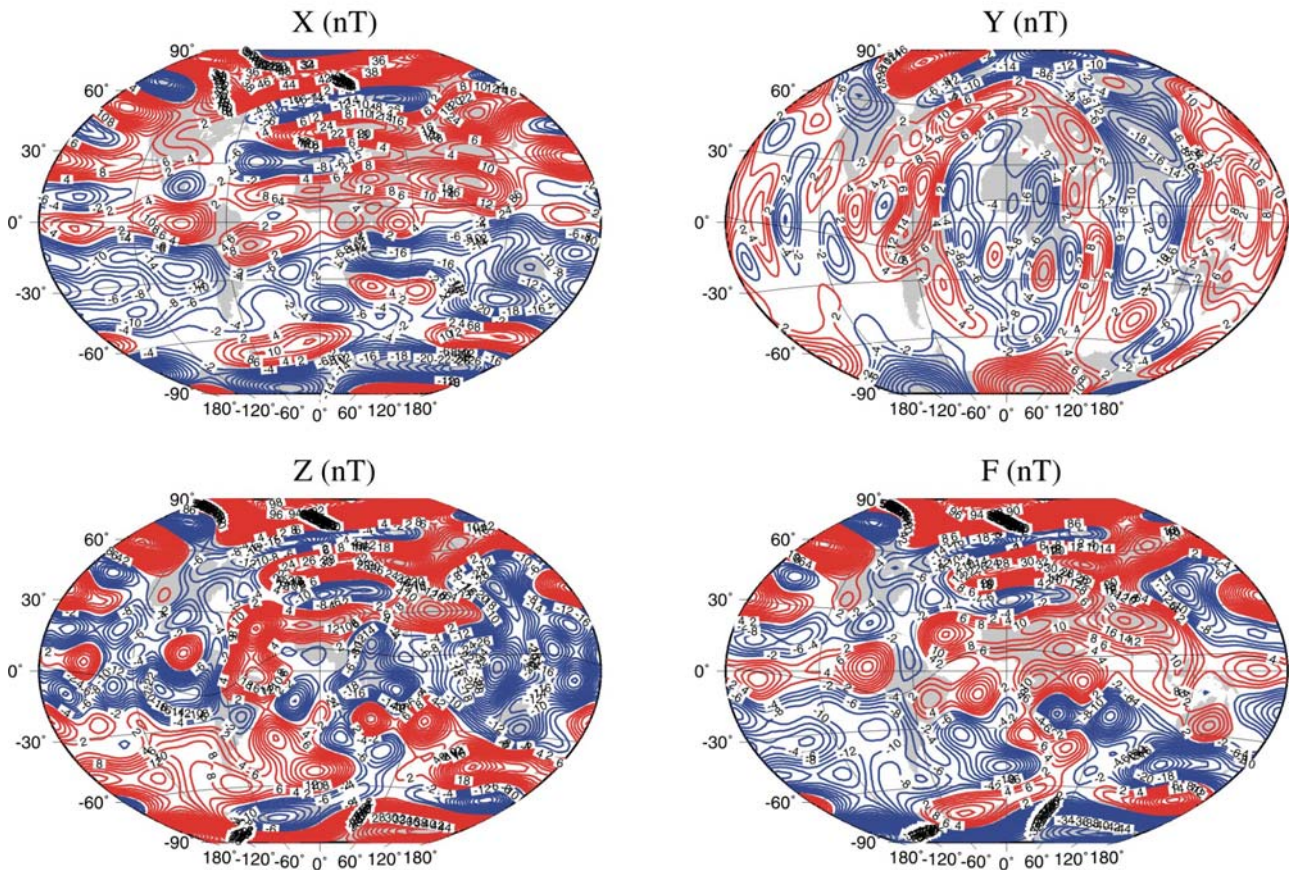


Figure 10

The amplitude of the differences in Figure 10, like Figure 9, is large and there are large differences in the polar regions. The common model where we see large differences in the polar regions is D1. The common model where we see large differences only at northern latitudes is C1.

Another concern is that the differences are not centred on zero and this may not be picked up when using the global mean RMS difference estimates of Figures 1-4. We have therefore computed the **mean** differences on a 2° latitude-longitude grid and the results are presented in Table 2.

Table 2 Mean differences (nT) in MF models on a 2° latitude-longitude grid at earth's surface

	X	Y	Z	F
A1-B3	0.1	0.0	-0.2	0.6
A1-C1	-2.0	0.0	-2.0	-3.6
A1-D1	0.2	0.0	5.2	-0.4
B3-C1	-2.1	0.0	-1.9	-4.2
B3-D1	0.1	0.0	5.3	-1.0
C1-D1	2.2	0.0	7.2	3.2

Table 2 can be summarised by model and this is given in Table 3.

Table 3 Mean of the mean differences (nT) in Table 2 for each MF model

	X	Y	Z	F
A1	-0.6	0.0	1.0	-1.1
B3	-0.6	0.0	1.1	-1.5
C1	-0.6	0.0	1.1	-1.5
D1	0.8	0.0	5.9	0.6

From Table 3 it can be seen that the differences are reasonably consistent for all MF models except for D1, particularly in Z.

The same analysis is now done for the SV models – see Tables 4 and 5.

Table 4 Mean differences (nT/year) in SV models on a 2° latitude-longitude grid at earth's surface

	X	Y	Z
A1-B3	-0.7	0.0	-2.2
A1-C1	-1.7	0.0	-1.1
A1-D1	0.7	0.0	0.0
B3-C1	-1.0	0.0	1.1
B3-D1	1.4	0.0	2.2
C1-D1	2.4	0.1	1.1

Table 5 Mean of the mean differences (nT/year) in Table 4 for each SV model

	X	Y	Z
A1	-0.6	0.0	-1.1
B3	-0.1	0.0	0.4
C1	-0.1	0.0	0.4
D1	1.5	0.0	1.1

From Table 5 it can be seen that the largest difference is that for X for SV model D1.

Whilst these analyses on latitude-longitude grids are very similar to computing global RMS differences using the Lowes-Mauersberger estimate, they highlight any mean differences across the globe and differences at high latitude. Comparisons with data have not been done because there are very few truly independent vector data. For example, after 2000.0 there are less than 500 vector observations from repeat stations submitted to WDC and the distribution globally is very poor.

4. Conclusions

The analyses presented here show that group D is producing models which are most different from the other models. The models produced by groups A-C are reasonably consistent with one another, with the exception of MF model C1 being different at northern latitudes and a zonal degree 4 signal in A1. Both groups A and B eliminate data with solar zenith angle $< 95^\circ$, C does not eliminate them but downweights them with the aim of achieving a reasonably even spatial distribution of data through time. This is important for data from the Ørsted satellite where the orbit drifts slowly with local time. Another explanation may be that group C includes more high latitude data than the other groups, with their use of observatory data. The zonal degree 4 signal in A1 is very probably due to the ionospheric leakage correction made in this model.

Whilst it can be argued that group D's approach is most different from the other groups, but nonetheless valid, they have used relatively few data to produce them and provided limited documentation at the time of submission. Comparisons between B1 and B2 show that there are large differences between models derived using data from just one satellite (RMS difference is 7.7 nT), so it is best to include data from all sources. Group D have only used data from the CHAMP satellite. We recommend that if their models are to be included, they be downweighted, particularly for the MF model.

Although SV model A1 is valid for 2005.0, by using it for characterizing SV at 2007.5 is equivalent to simply ignoring secular acceleration after this date. With two other models incorporating quadratic polynomial extrapolation to 2007.5, using a simple averaging to get the final IGRF SV model will result in a good compromise.